



MX070081

INFORME TECNICO  
ACEL-8603 FEBRERO/1986

OSCILACIONES EN LA FUSION DE SISTEMAS DE Si + Si.  
E.F. Aguilera, J.J. Kolata, P.A. DeYoung, J.J. Vega.

Proyecto BZ23A  
Departamento del Acelerador  
Gerencia de Investigación Básica  
Dirección de Técnicas Nucleares  
I.N.I.N.

(Plática dada en el IX Simposium de Física Nuclear en Oaxtepec,  
Enero de 1986)

## OSCILACIONES EN LA FUSION

DE SISTEMAS DE  $Si+Si$

E. F. Aguilera

Centro Nuclear, ININ, Apdo. Postal 18-1027, México, D. F.

J. J. Kolata, P. A. DeYoung and J. J. Vega

Physics Department, University of Notre Dame

Notre Dame, In. 46556

### RESUMEN

Usando técnicas de rayos  $\gamma$ , se midieron funciones de excitación para todos los núcleos residuales de las reacciones  $^{28}Si+^{28,30}Si$  y  $^{30}Si+^{30}Si$ , para energías en el centro de masa entre una y dos veces la barrera Coulombiana. Trece elementos fueron identificados para la primera reacción y diez para las otras dos. Mientras ninguna estructura es mostrada por los datos para la reacción  $^{28}Si+^{28}Si$ , hemos encontrado evidencia de estructura intermedia en los canales  $2\alpha$  y  $\alpha p n$  en  $^{28}Si+^{30}Si$  y de estructura gruesa en la sección eficaz de fusión total para  $^{30}Si+^{30}Si$ . Cálculos usando un modelo de penetración de barrera con un parámetro libre reproducen los resultados experimentales muy bien. Cálculos de un modelo de evaporación indican que la estructura individual de los núcleos que aparecen en las cadenas de decaimiento pueden tener una influencia importante sobre el proceso de desexcitación a las energías relevantes en nuestros experimentos.

(Talk delivered at Oaxtepec Meeting Jan. 1986)

OSCILLATIONS IN THE FUSION OF

Si+Si SYSTEMS

E. F. Aguilera

Centro Nuclear, ININ, Apdo. Postal 18-1027, México, D. F.

J. J. Kolata, P. A. DeYoung and J. J. Vega

Physics Department, University of Notre Dame

Notre Dame, In. 46556

ABSTRACT

Excitation functions for the yields of all the residual nuclei from the  $^{28}\text{Si}+^{28,30}\text{Si}$  and  $^{30}\text{Si}+^{30}\text{Si}$  reactions have been measured via the  $\gamma$ -ray technique for center of mass energies in the region within one and two times the Coulomb barrier. Thirteen elements were identified for the first reaction and ten for the other two. While no structure is shown by the data for the  $^{28}\text{Si}+^{28}\text{Si}$  reaction, we have found evidence for intermediate width structure in the  $2\alpha$  and the  $\alpha_{pn}$  channels in  $^{28}\text{Si}+^{30}\text{Si}$  and for broad structure in the total fusion cross sections for  $^{30}\text{Si}+^{30}\text{Si}$ . Calculations using a barrier penetration model with one free parameter reproduce the experimental results quite well. Evaporation model calculations indicate that the individual structure of the nuclei involved in the respective decay chains might have an important influence upon the deexcitation process at the energies relevant to our experiments.

## I INTRODUCTION

One of the features of fusion not yet well understood is the presence of oscillations in the fusion excitation functions observed for several light heavy-ion reactions <sup>1-4</sup>. Theoretical attempts have been made to explain the gross oscillations for a few systems but often the same data sets are equivalently described with the predictions of rather antagonistic models <sup>5-7</sup>. Thus, possible interpretations of the phenomenon include its association with shape resonances of grazing partial waves in the entrance channel <sup>5</sup> on one hand and the assumption that it can be explained in terms of the properties of the level density in the compound nucleus <sup>6,7</sup> on the other hand.

It is not clear at present which of these models, if any, is the correct one and therefore it is important to have sufficient experimental information on as many systems as possible in order to achieve a better understanding of the phenomenon. Although systematic studies along these lines have been performed for many different combinations of target-projectile (4,8,9 and Refs. therein), most of these are rather light heavy-ions and in fact only scarce experimental work has been done in the region of compound nuclei with  $A \gtrsim 50$ .

In recent publications <sup>10,11</sup>, we reported the results of a systematic investigation of fusion for the systems  $^{28}\text{Si} + ^{28,30}\text{Si}$  and  $^{30}\text{Si} + ^{30}\text{Si}$ , all of which fall into this not-well-studied mass region. The main features of these results are described here

along with an additional analysis of the corresponding evaporation stage for each reaction.

The observed trend to favor structure in the fusion of identical  $\alpha$ -particle nuclei<sup>4</sup> makes the  $^{28}\text{Si}+^{28}\text{Si}$  system a particularly interesting case to study. In addition, the fact that a surface-transparent optical potential has been suggested to describe the observations for the corresponding elastic channel<sup>12</sup>, increases the expectation that oscillations may appear in the fusion cross sections<sup>4,5</sup>. Some scarce evidence for this kind of oscillations has been reported in Ref. 13 but more data were clearly needed in order to make conclusive statements. The possibility of having fusion data obtained with deformed ions such as  $^{28}\text{Si}$  and  $^{30}\text{Si}$ , adds some interest to the present study.

After describing the experimental method in section II, we present the results in section III. Then, a comparison with evaporation model calculations is made in section IV and, finally, a summary and the conclusions of this work are presented in section V.

## II EXPERIMENTAL METHOD

Beams of  $^{28}\text{Si}$  and  $^{30}\text{Si}$  were obtained with the 3-stage Van de Graaff facility at the University of Notre Dame. For each reaction, excitation functions were obtained with steps of 500 keV in the lab system for center of mass energies in the region between one and two times the Coulomb barrier. The  $^{28}\text{Si}$

target (99.9%) was  $35 \mu\text{g}/\text{cm}^2$  thick while for the  $^{30}\text{Si}$  target (95.2%) the thickness was  $24 \mu\text{g}/\text{cm}^2$ . They both were deposited onto a thick Au backing and then covered with a thin Au layer to retard oxidation.

The total yields of  $\gamma$ -rays emitted by the evaporation residues were determined by placing a Ge(Li) detector at  $125^\circ$  to the beam. Observed deviations in the collected charge were corrected for by assuming a smooth energy behavior of the Coulex of  $\gamma$ -ray lines from the Au backing. The absolute normalization was obtained by using an appropriate scaling procedure, as illustrated in table 1 for the case of  $^{28}\text{Si}+^{30}\text{Si}$  and  $^{30}\text{Si}+^{30}\text{Si}$ . The estimated uncertainty in this normalization (not included in the error bars of the figures) was 10% for these two reactions and 9% for  $^{28}\text{Si}+^{28}\text{Si}$ .

The reactions  $^{28}\text{Si}+^{16}\text{O}$  and  $^{30}\text{Si}+^{16}\text{O}$  were also measured at the same energies as in the previous experiments in order to correct the effects of oxygen contamination of our targets. Activity contamination of our spectra was also corrected for with the help of beam-off spectra recorded after prolonged bombardement of the targets.

Production cross sections for the reaction residues were determined from  $\gamma$ -ray yields corresponding to the respective ground state transitions (or approximations to them), as indicated in table 2. Further details of the experimental procedure have been extensively described elsewhere <sup>11,15</sup>.

### III RESULTS

Thirteen residual nuclei were identified as resulting from the  $^{28}\text{Si}+^{28}\text{Si}$  reaction and ten for the case of  $^{28,30}\text{Si}+^{30}\text{Si}$ . Excitation functions for selected residues are presented in Figs. 1-3. The complete set of experimental results has been previously reported<sup>11,15</sup>.

None of the excitation functions for individual evaporation channels in the  $^{28}\text{Si}+^{28}\text{Si}$  experiment showed a behavior that could be considered as a nonstatistical oscillation. In particular, the possible structures in the  $^{50}\text{Cr}$  excitation function at 92 and 97 MeV reported by DiCenzo et al.<sup>13</sup> are not seen in our data, presented in Fig. 1, in spite of the smaller energy steps. These authors found indications of correlated structure at these two energies for the transitions at 610, 783, 1098 and 1283 keV in  $^{50}\text{Cr}$ . The possible presence of  $^{50}\text{Mn}$  in the reaction<sup>15,16</sup> would offer an explanation for this since the last three lines are present in the decay of this nuclide. The energies at which a "structure" originating in the decay is observed would then depend on the detailed history of the experiment, which in turn would explain why we did not see such structure. Alternatively, the results observed in Ref. 13 could be the effect of purely random fluctuations, as the same authors have pointed out.

For the case of the  $^{28}\text{Si}+^{30}\text{Si}$  experiment an apparent structure is observed in Fig. 2 for the  $2\alpha$  ( $^{52}\text{Mn}$ ) and the  $\alpha\text{pn}$  ( $^{50}\text{Cr}$ ) channels, both of which show a sharp peak at 83.5 MeV.

A correlation analysis was made including the lines at 783, 1098 and 1283 keV in  $^{50}\text{Cr}$  and those at 870 and 930 keV in  $^{52}\text{Mn}$ , the more statistically significant lines in these nuclides.

The cross correlation function  $^{11}$ , presented in Fig. 4, shows an actual correlation at 83.5 MeV, where the respective value differs from zero by more than four standard deviations. Other possible (weaker) correlated structure becomes evident in this figure at 89, 90.5 and 92 MeV, but the cross correlation function differs from zero by only a little more than two standard deviations at these energies. It would be highly desirable to have more points in this energy region, with better statistics, in order to corroborate the presence of this seemingly rich structure.

The excitation function for  $^{57}\text{Co}$ , one of the most prominent residues from the  $^{30}\text{Si}+^{30}\text{Si}$  reaction, is presented in Fig. 3. No structure that could be resolved within the 5% error bars is observed here and the same is true for all the other evaporation channels in this reaction. However, a broad structure appears in the excitation function for the total fusion cross section, as shown in the lower part of Fig. 5. Here, a fluctuation of about 10% with respect to the average behavior becomes apparent in the region above 36 MeV cm energy. This structure is reminiscent of that observed  $^{17}$  in  $^{16}\text{O}+^{16}\text{O}$ , which is probably related to shape resonances in the entrance channel.

The curves in Fig. 5 correspond to a barrier penetration model calculation in which the barrier in the effective potential



(Coulomb+nuclear+centrifugal) is approximated by an inverted parabola. In this model <sup>18</sup>, the equivalent sharp surface radius used in the nuclear proximity potential is modified by an additive parameter  $\Delta R$ , which is varied until a good match to the data is obtained. The height ( $V_0$ ), radius ( $R_0$ ) and curvature ( $R\omega_0$ ) of the fusion barrier can be found with this procedure and these parameters are shown in table 3 along with a comparison with empirical trends <sup>18</sup> for the reduced parameters

$$r_{ef} = Z_T Z_P e^2 / V_0 (A_T^{1/3} + A_P^{1/3}) \quad \text{and}$$

$$r_{of} = R_0 / (A_T^{1/3} + A_P^{1/3}) \quad .$$

It is clear from the table that the barrier parameters obtained in this work follow the systematic trends quite well.

#### IV COMPARISON WITH EVAPORATION MODEL CALCULATIONS

Evaporation calculations were made within the Hauser-Feshbach formalism by using the code CASCADE <sup>19</sup>. Four reasonable sets of parameters were tried <sup>15</sup> for the case of  $^{28}\text{Si} + ^{28}\text{Si}$  at  $E_{cm} = 45$  MeV and the best one was selected to do the calculations for all energies in the three reactions studied.

The results of these calculations for the  $^{28}\text{Si} + ^{28}\text{Si}$  system are compared to the experimental data in Fig. 6. A good agreement is observed here for two of the most important channels,  $^{50}\text{Cr}(\alpha 2p)$  and  $^{53}\text{Mn}(3p)$ , and for the weak channel  $^{54}\text{Fe}(2p)$ . On the other hand, the agreement of predicted and experimental trends is only fair for the two intermediate-strength channels

$^{47}\text{V}(2\alpha\text{p})$  and  $^{53}\text{Fe}(2\text{pn})$ , and is rather poor for all remaining channels, including the strong  $^{49}\text{V}(\alpha 3\text{p})$  channel.

Careful inspection of Fig. 6 for the residues where one  $\alpha$ -particle was evaporated suggests to make a grouping for the  $\alpha\text{p}$ ,  $\alpha\text{pn}$ ,  $\alpha 2\text{pn}$  and  $\alpha 3\text{p}$  evaporation channels. The sum of the experimental yields for these channels is compared to the corresponding theoretical cross sections in Fig. 7, where the predictions for each individual channel are also included. The substantial improvement observed in the agreement indicates that CASCADE is not modeling the  $\alpha\text{p}(x \text{ nucleons})$  emission properly, i.e., the decay chain that according to CASCADE terminates in  $^{50}\text{Mn}(\alpha\text{pn})$  or in  $^{51}\text{Mn}(\alpha\text{p})$  is actually going on to  $^{49}\text{Cr}(\alpha\text{p}\{\text{pn}\})$  and  $^{49}\text{V}(\alpha\text{p}\{2\text{p}\})$ . Whether the reason for this lies in the potentials used in the optical model or is related to the treatment of the level densities cannot be concluded from the present work.

The same compound nucleus  $^{56}\text{Ni}$  has been analyzed in detail at higher excitation energy (83 MeV) by Pühlhofer et al.<sup>20</sup>, who obtained fairly good agreement between prediction and experiment for the detailed nuclide distributions. Since essentially the same set of parameters was used in our work, the discrepancies observed in Fig. 6 could indicate that the respective calculations are more sensitive to the individual structure of the nuclei involved in the decay for the lower excitation energies relevant to our experiment.

The overall agreement of experimental and theoretical

trends and magnitudes is better for the  $^{28}\text{Si}+^{30}\text{Si}$  data presented in Fig. 8 than it was for  $^{28}\text{Si}+^{28}\text{Si}$ . The  $^{30}\text{Si}+^{30}\text{Si}$  data shown in Fig. 9 could be qualified as intermediate between these two. It is interesting to note that all the systems analyzed in the work of Ref. 20, for which good quality predictions were reported, corresponded to asymmetric entrance channels.

The fact that  $^{54}\text{Fe}$  is one of the most important decay residues for both the  $^{58}\text{Ni}$  (Fig. 8) and the  $^{60}\text{Ni}$  (Fig. 9) compound nuclei and that its yield is badly underpredicted in both cases, could indicate the presence of some peculiar high-spin state in  $^{54}\text{Fe}$  which is attracting a considerable amount of cross section that could not be accounted for by the calculations. More work is needed in order to corroborate this hypothesis.

#### V SUMMARY AND CONCLUSIONS

the fusion of the three systems  $^{28}\text{Si}+^{28},^{30}\text{Si}$  and  $^{30}\text{Si}+^{30}\text{Si}$  has been studied in this work via the  $\gamma$ -ray technique. Thirteen residues were identified for the first reaction and ten for the other two.

The possibility of oscillations for the  $^{28}\text{Si}+^{28}\text{Si}$  system, suggested by the results of previous observations, was ruled out here as no structure that could be resolved within the 3% error bars was observed in our work. A possible delayed decay was suggested to account for the different observations.

In the case of the  $^{28}\text{Si}+^{30}\text{Si}$  reaction, a correlated structure at 83.5 MeV, having a peak to valley ratio of more than 15% and a width of about 1 MeV, was observed for the  $2\alpha$  and  $\alpha p n$  channels. Evidence for more structure (weaker) of about the same width was also found for the same channels in the region above this energy.

No obvious structure appeared in the yields for individual residues from the  $^{30}\text{Si}+^{30}\text{Si}$  reaction, but a broad oscillation was observed in the total fusion cross section extending from about 36 to 42.5 MeV cm energy, showing a fluctuation of about 10% with respect to the average behavior. This reminds one of the similar structure observed in lighter identical-particle systems, with which could share a common origin.

The general trends of our data are well described by the predictions of a simple barrier penetration model. By varying only one parameter, empirical barrier parameters are extracted which follow very well the systematic trends obtained from a large number of other reactions.

Some discrepancies were observed between the predictions of the statistical model and the experimental mass and charge distributions measured in this work, with the asymmetric system giving the best overall agreement. It is possible that the individual structure of the nuclei involved might be playing an important role in determining the deexcitation process at the excitation energies relevant to our experiments.

In conclusion, our results seem to indicate that the observed tendency for preferential structure in the fusion of identical nuclei is not valid for Si+Si systems. Further experimental work suggested by this study would include a more detailed investigation of  $^{28}\text{Si}+^{30}\text{Si}$  in the region between 40 and 50 MeV cm energy, where a rich structure is apparent in our data. It would be also very interesting to extend our measurements on  $^{30}\text{Si}+^{30}\text{Si}$  to higher energies, where additional oscillatory behavior might be expected from our results.

## R E F E R E N C E S

- 1.- W. Henning, Dynamics of Heavy Ion Collisions, eds. N. Cindro et al., North Holland, 75 (1981).
- 2.- Resonances in Heavy Ion Reactions, Lecture Notes in Physics 156, Springer Verlag (1982).
- 3.- T.M. Cornier, Ann. Rev. Nucl. and Part. Sci. 32, 271 (1982).
- 4.- K.A. Erb and D.A. Bromley, Treatise on Heavy-Ion Science, vol. 3, p. 201, Ed. D.A. Bromley, Plenum (1985).
- 5.- Y. Kondo, D.A. Bromley and Y. Abe, Phys. Rev. C22, 1068 (1980).
- 6.- R. Vandenbosch, Phys. Lett. 87B, 183 (1979).
- 7.- R. Vandenbosch and A. J. Lazzarini, Phys. Rev. C23, 1074 (1981).
- 8.- D.G. Kovar, D.F. Geesaman, T.H. Braid, Y. Eisen, W. Henning, T.R. Ophel, M. Paul, K.E. Rehm, S.J. Sanders, P. Sperr, J.P. Schiffer, S.L. Tabor, S. Vigdor, B. Zeidman and F.W. Prosser, Jr., Phys. Rev. C20, 1305 (1979).
- 9.- J.J. Kolata, R.A. Racca, P.A. De Young, E. Aguilera-Reyes and M.A. Xapsos, Phys. Rev. C32, 1080 (1985).
- 10.- E.F. Aguilera, J.J. Kolata, J.D. Hinnefeld, L.J. Satkowiak, J.J. Vega and P.A. De Young, Bull. Am. Phys. Soc. 28, 979 (1983).
- 11.- E.F. Aguilera, J.J. Kolata, P.A. De Young and J.J. Vega, submitted to Phys. Rev. C.
- 12.- R.R. Betts, S.B. DiCenzo and J.F. Petersen, Phys. Rev. Lett. 43, 253 (1979).
- 13.- S.B. DiCenzo, J.F. Petersen and R.R. Betts, Phys. Rev. C23, 2561 (1981).
- 14.- J.J. Kolata, R.M. Freeman, F. Haas, B. Heusch and A. Gallman, Phys. Rev. 65B, 333 (1976).
- 15.- E.F. Aguilera, Ph.D. Dissertation, University of Notre Dame (1981).
- 16.- L.R. Medsker, L.V. Theisen, L.H. Fry, Jr. and J.S. Clements, Phys. Rev. C, 790 (1979).
- 17.- J.J. Kolata, R.C. Fuller, R.M. Freeman, F. Haas, B. Heusch and A. Gallman, Phys. Rev. C16, 891 (1977).
- 18.- L.C. Vaz, J.M. Alexander and G.R. Satchler, Phys. Rev. C9, 373 (1981).
- 19.- Puhlhofer, F. Nucl. Phys. A280 (1977) 267.
- 20.- Puhlhofer, F., Schneider, W.F.W., Busch, F. Barrete, J., Braun Munzinger, P. Gelbke, C.K. and Wegner, H.E., Phys. Rev. C16 (1977) 1010.

TABLE 1

Experiments performed to determine the absolute normalization for  $^{28}\text{Si}+^{30}\text{Si}$  and  $^{30}\text{Si}+^{30}\text{Si}$ . All absolute cross sections are referred to the values measured by Kolata et al.<sup>14</sup> (1976) for  $^{16}\text{O}+^{12}\text{C}$ .

Projectile	Target	$E_{\text{cm}}$ (MeV)	$\gamma$ -ray lines analyzed $E_{\gamma}$ (keV)	Outcome from the analysis
$^{16}\text{O}$	$^{12}\text{C}$	19.29, 24.86	1634 ( $^{20}\text{Ne}$ )	Target thickness
$^{30}\text{Si}$	$^{12}\text{C}$	20.46, 22.86	892 ( $^{40}\text{K}$ )	$\sigma_{\text{abs}}$ for $^{30}\text{Si}+^{12}\text{C}$
$^{12}\text{C}$	$^{30}\text{Si}$	20.46, 22.86	892 ( $^{40}\text{K}$ )	Target thickness
$^{28}\text{Si}$	$^{30}\text{Si}$	42.18	606 ( $^{55}\text{Fe}$ ) 1097 ( $^{50}\text{Cr}$ )	$\sigma_{\text{abs}}$ for $^{28}\text{Si}+^{30}\text{Si}$
$^{30}\text{Si}$	$^{30}\text{Si}$	35.82, 40.00	411 ( $^{54}\text{Fe}$ )	$\sigma_{\text{abs}}$ for $^{30}\text{Si}+^{30}\text{Si}$

TABLE 2

Identified residues and gamma-ray lines used to obtain the corresponding excitation functions

<u>RESIDUE</u>	<u>LINES USED (keV)</u>	<u>N O T E S</u>
46Ti	888(a)	(i)
47V	1148	(i)
48V	427,626(b)	(i)
48Cr	751	(i)
49V	1021	(i), (ii,d)
49Cr	271,1084(b)	(i), (ii,d,e)
50Cr	782	(i,a), (ii,a,d), (iii,d)
51Cr	1163,1480	(i), (ii,d), (iii,b,d)
52Cr	1434	(ii,f), (iii,d)
51Mn	237(c), 1139(b)	(i)
52Mn	870,2286(b)	(ii,d)
53Mn	1440	(i), (ii,d), (iii,d)
54Mn	213	(ii), (iii,d)
53Fe	700(c)	(i)
54Fe	1409(a)	(i), (ii,c), (iii,d)
55Fe	1317	(ii,b), (iii,b,d)
56Fe	846	(iii)
57Fe	870,992,1061	(iii)
57Co	1223,1690	(iii,b)

(i) Analyzed in  $^{28}\text{Si}+^{28}\text{Si}$

(ii) Analyzed in  $^{28}\text{Si}+^{30}\text{Si}$

(iii) Analyzed in  $^{30}\text{Si}+^{30}\text{Si}$

(a) A contribution from 0 contamination was subtracted

(b) This determination involves reported branchings ratios

(c) A correction for activity from a long lived state was made

(d) A contribution from  $^{28}\text{Si}$  contaminant was subtracted

(e) The yield in the 271 keV line was estimated by the sum of the yields in the lines at 812 and 1289 keV, corrected for 0-cont.

(f) The 1163 keV line was used instead of the one at 1434 keV.



TABLE 3

Empirical parameters obtained from our data using the  
Barrier Penetration Model  
 $\Delta R$ -fitting par.,  $R_0$ ,  $V_0$ ,  $\hbar\omega_0$  - radius, height and curvature of barrier  
 $r, \bar{r}$  - radius parameters (see text) and corresponding systematic trends

System	$\Delta R$ (fm)	$R_0$ (fm)	$V_0$ (MeV)	$\hbar\omega_0$ (MeV)	$r_{ef}/\bar{r}_{ef}$	$r_{of}/\bar{r}_{of}$
$^{28}\text{Si}+^{28}\text{Si}$	0.15	8.94	28.89	3.42	0.99	0.99
$^{28}\text{Si}+^{30}\text{Si}$	0.08	8.86	29.13	3.39	0.98	0.97
$^{30}\text{Si}+^{30}\text{Si}$	0.11	9.06	28.54	3.26	0.98	0.97

#### FIGURE CAPTIONS

- FIG. 1. Experimental excitation function for production of  $^{50}\text{Cr}(\alpha 2p)$  from the  $^{28}\text{Si}+^{28}\text{Si}$  reaction.
- FIG. 2. Experimental excitation functions for production of  $^{52}\text{Mn}(\alpha pn)$  and  $^{50}\text{Cr}(2\alpha)$  from the  $^{28}\text{Si}+^{30}\text{Si}$  reaction. A correlated structure is observed at 83.5 MeV, as indicated by the arrows.
- FIG. 3. Experimental excitation function for production of  $^{57}\text{Co}(p2n)$  from the  $^{30}\text{Si}+^{30}\text{Si}$  reaction.
- FIG. 4. Cross correlation function for the yields of the lines at 870 and 930 keV in  $^{52}\text{Mn}$  and the lines at 783, 1098 and 1283 keV in  $^{50}\text{Cr}$ , as measured in the  $^{28}\text{Si}+^{30}\text{Si}$  experiment.
- FIG. 5. Total fusion cross sections obtained in our experiments (crosses) and comparison with predictions of barrier penetration model (dashed lines).
- FIG. 6. Excitation functions for evaporation residues from  $^{28}\text{Si}+^{28}\text{Si}$ . The solid lines follow the experimental points while the black dots are the results of CASCADE calculations.
- FIG. 7. Comparison of experimental and theoretical excitation functions for products of the  $\alpha px$  emission chain in the  $^{28}\text{Si}+^{28}\text{Si}$  system.
- FIG. 8. Same as Fig. 6 but for the  $^{28}\text{Si}+^{30}\text{Si}$  system.
- FIG. 9. Same as Fig. 6 but for the  $^{30}\text{Si}+^{30}\text{Si}$  system.

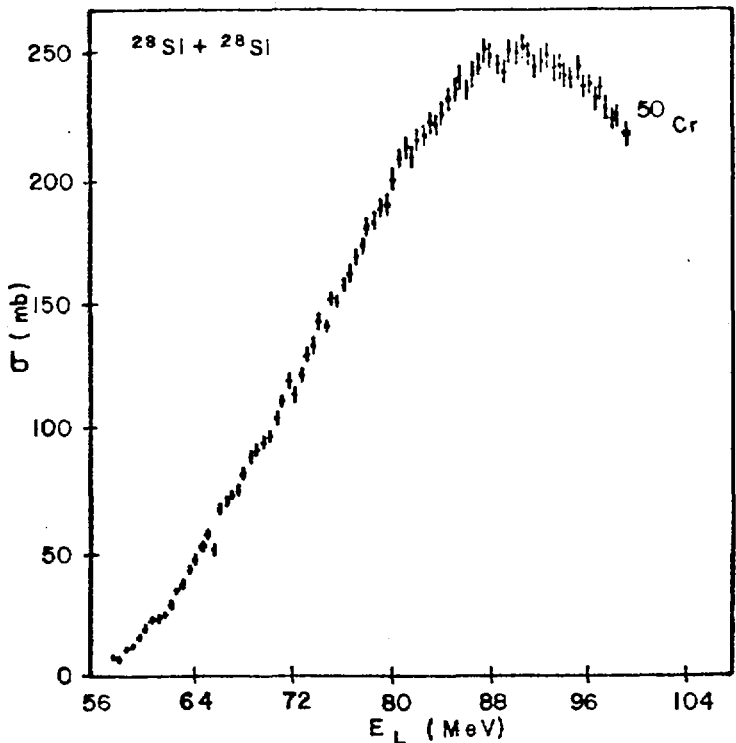


FIGURE 1

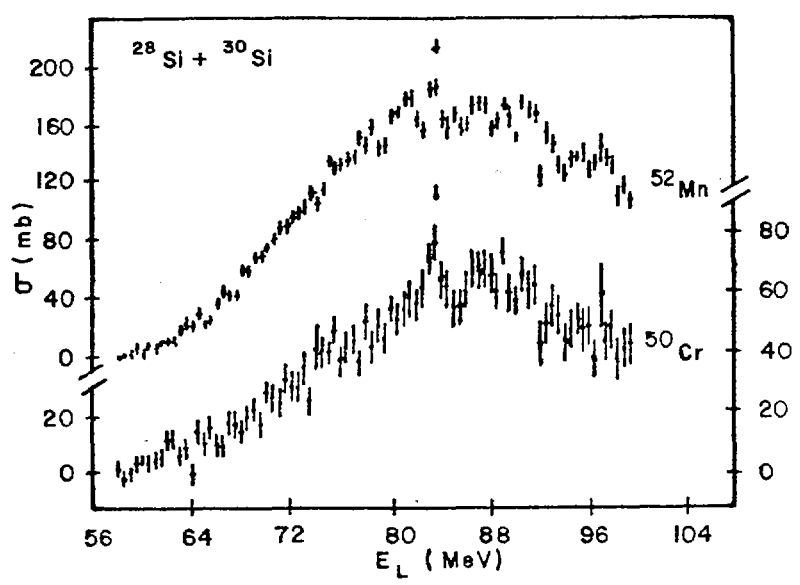


FIGURE 2

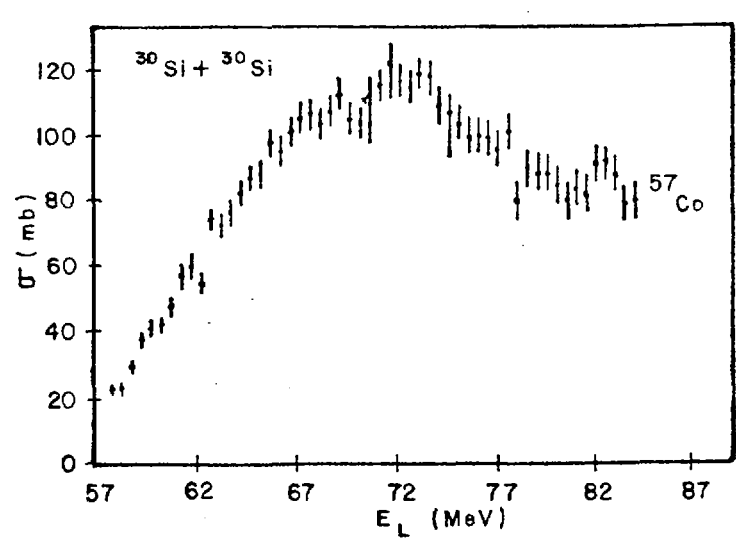


FIGURE 3

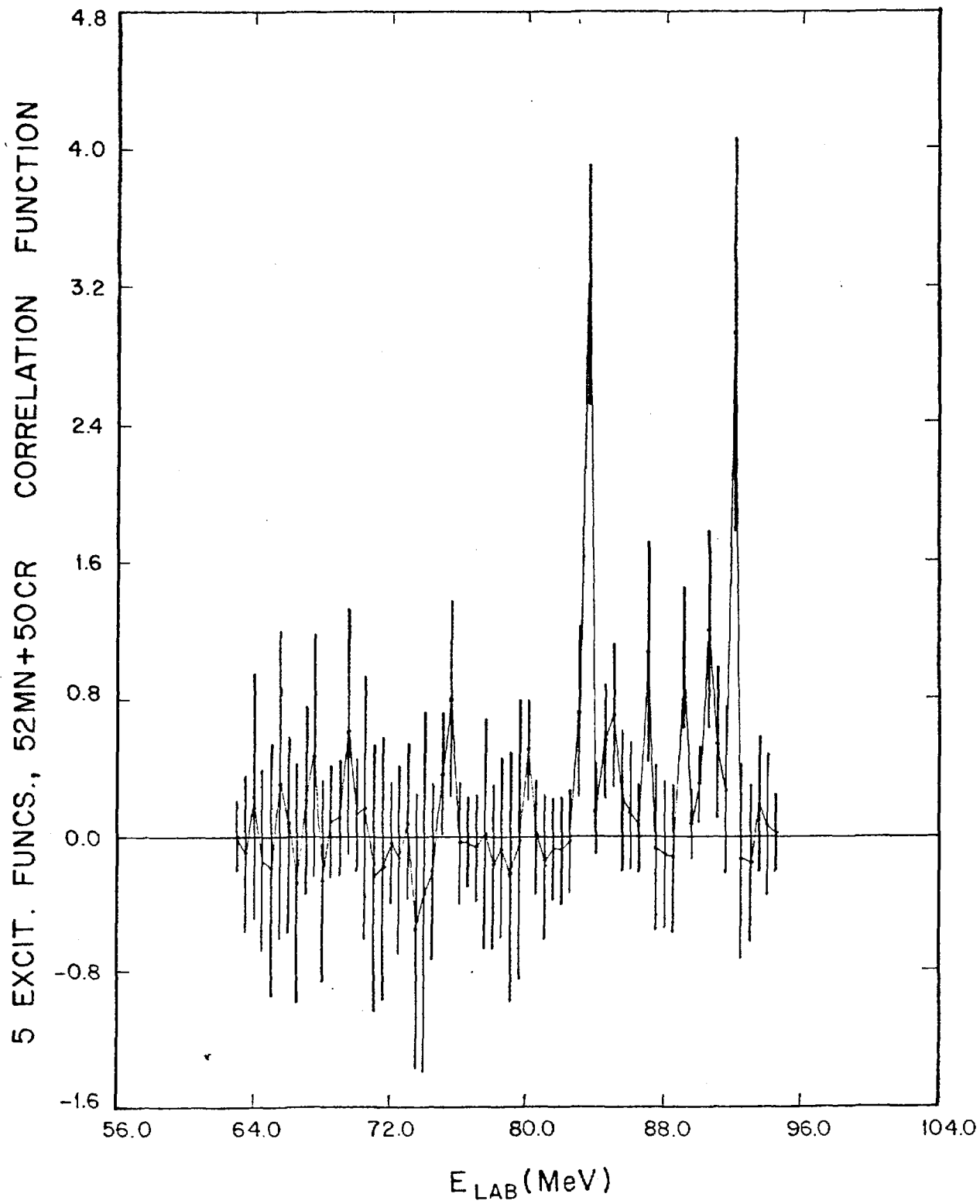


FIGURE 4

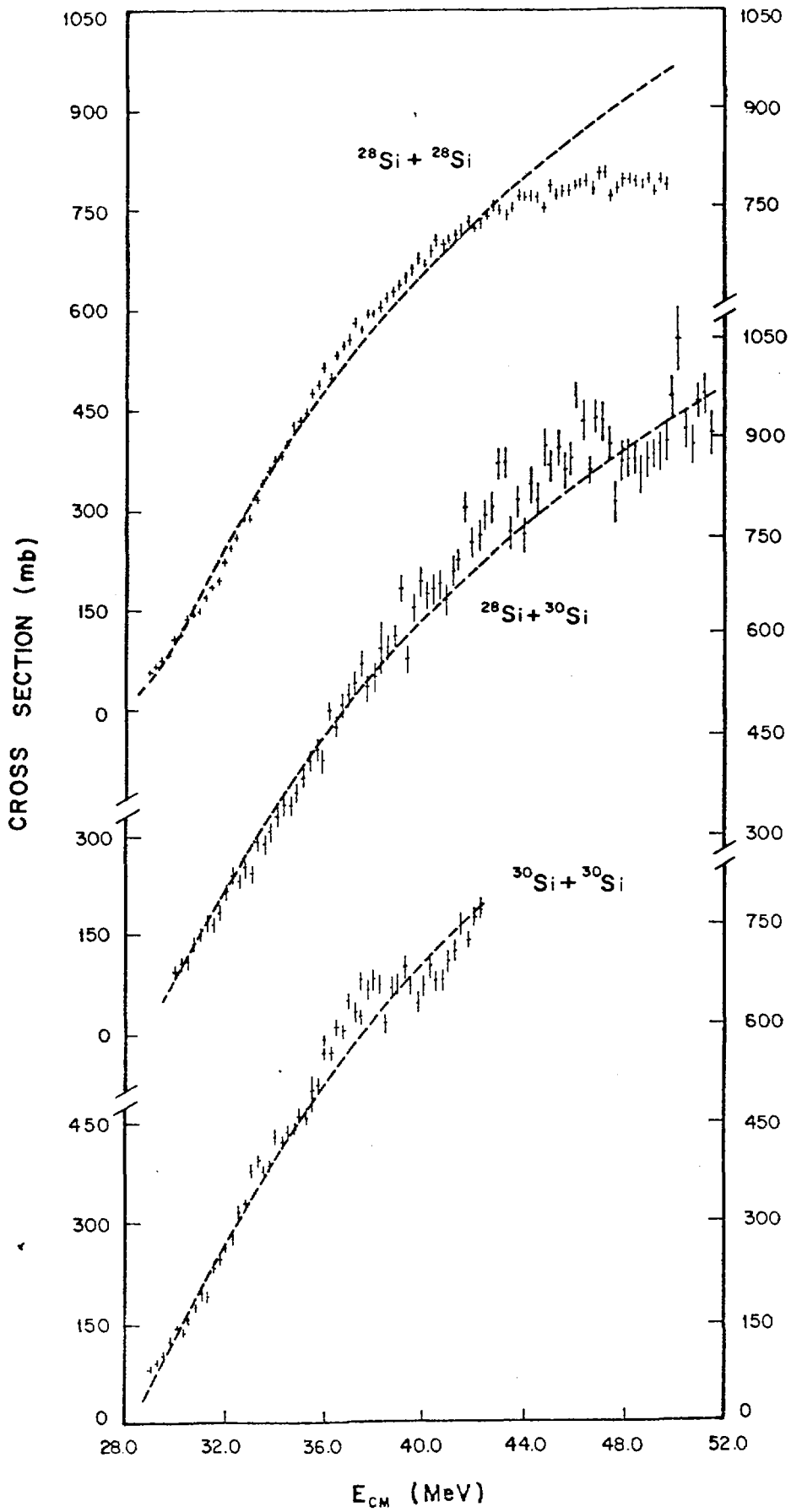


FIGURE 5

EXCITATION FUNCTIONS FOR EVAPORATION RESIDUES FROM  $^{28}\text{Si} + ^{28}\text{Si}$

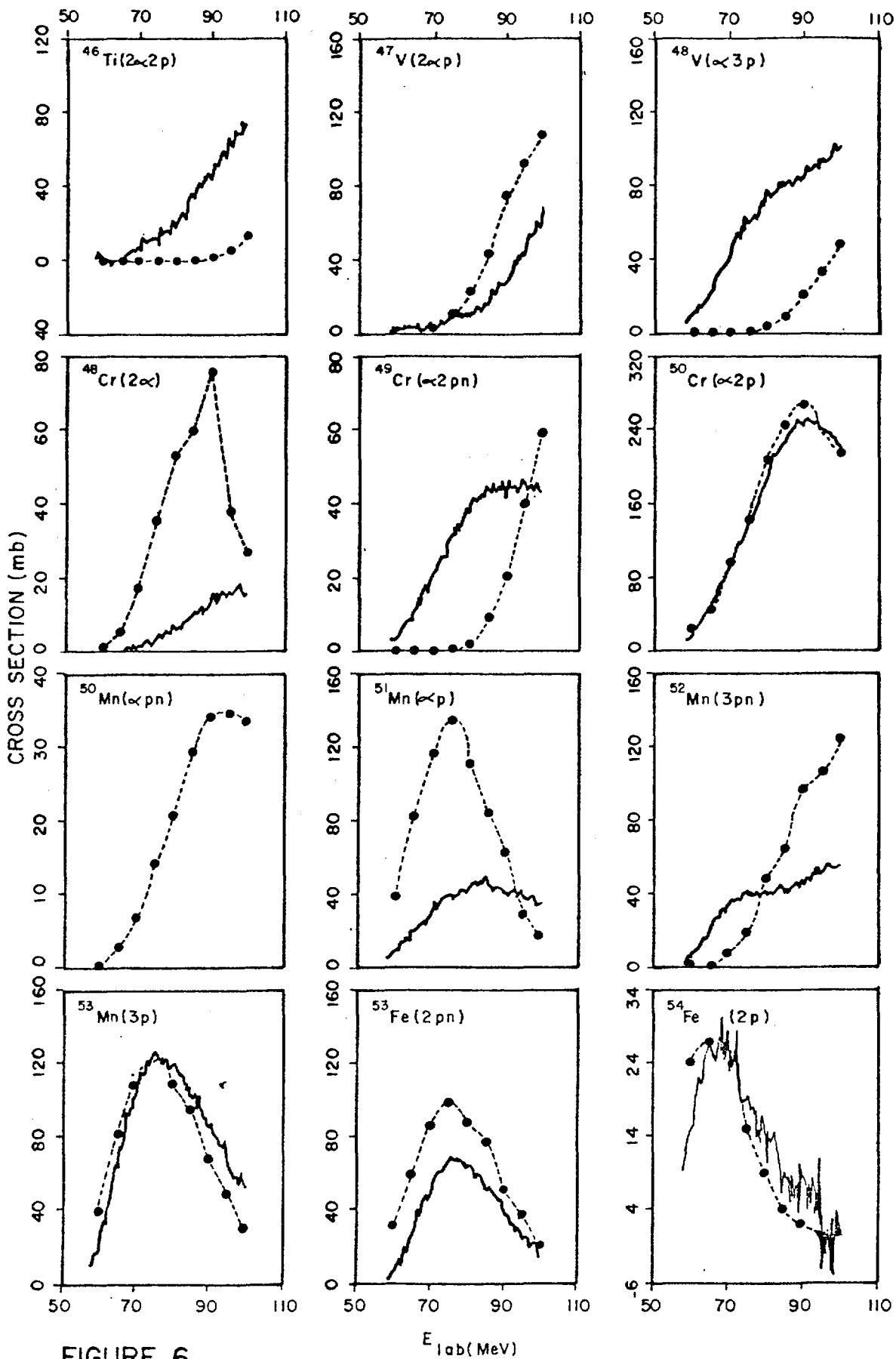


FIGURE 6

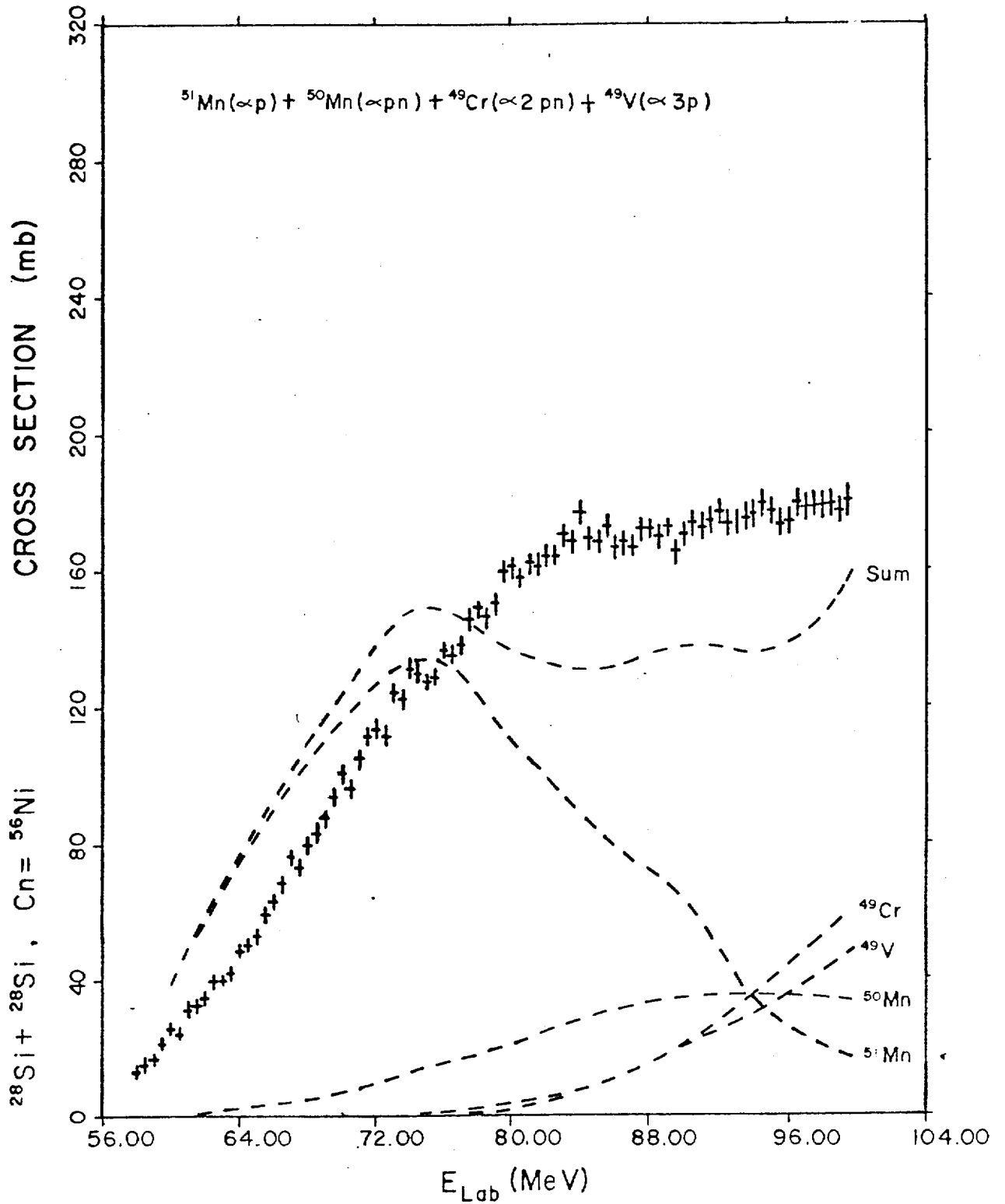


FIGURE. 7

COMPARISON OF EXPERIMENT (CROSSES) WITH  
CASCADE CALCULATIONS (DASHED LINE)

EXCITATION FUNCTIONS FOR EVAPORATION RESIDUES FROM  $^{28}\text{Si} + ^{30}\text{Si}$

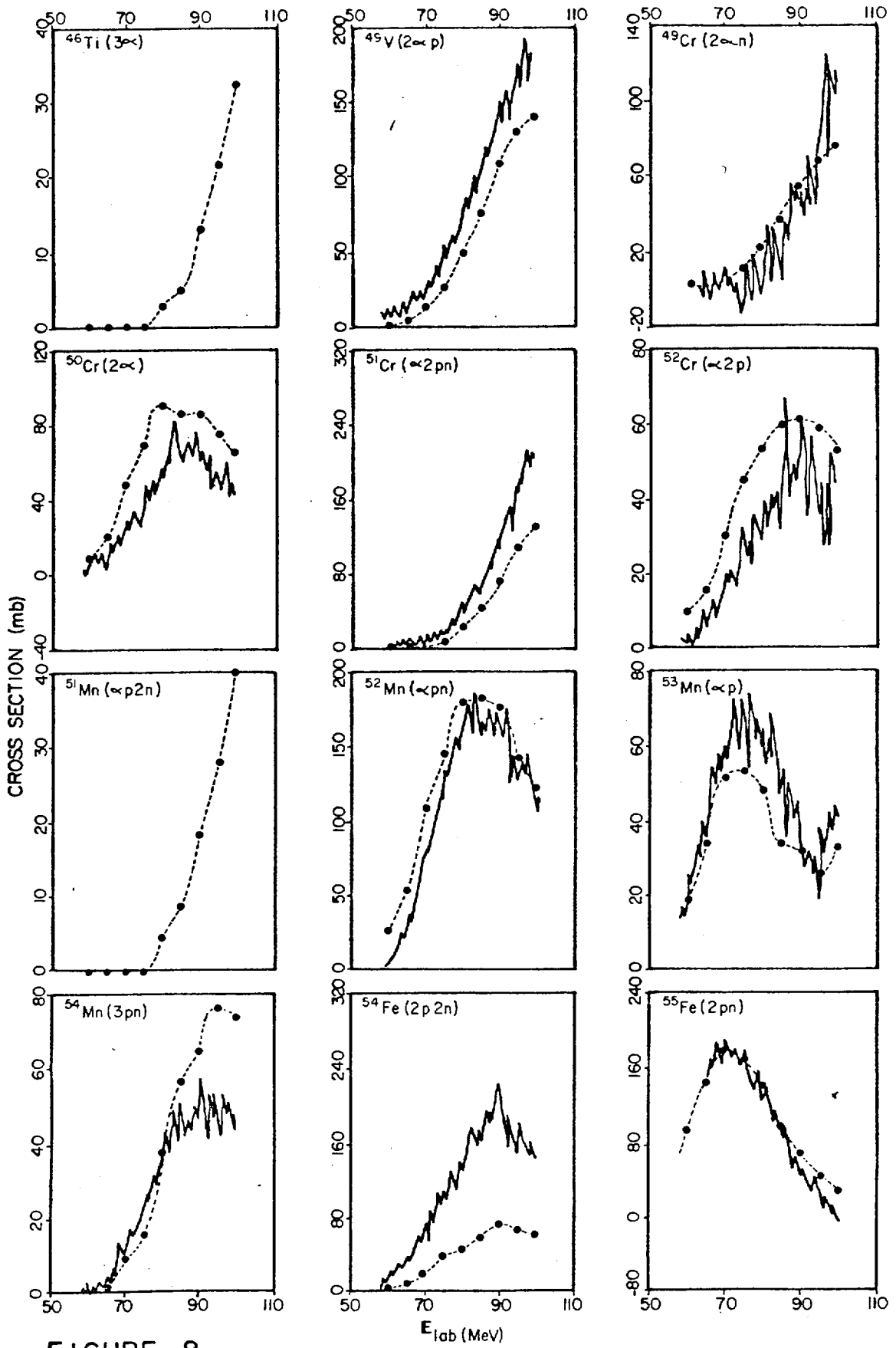


FIGURE 8



EXCITATION FUNCTIONS FOR EVAPORATION RESIDUES FROM  $^{30}\text{Si} + ^{30}\text{Si}$

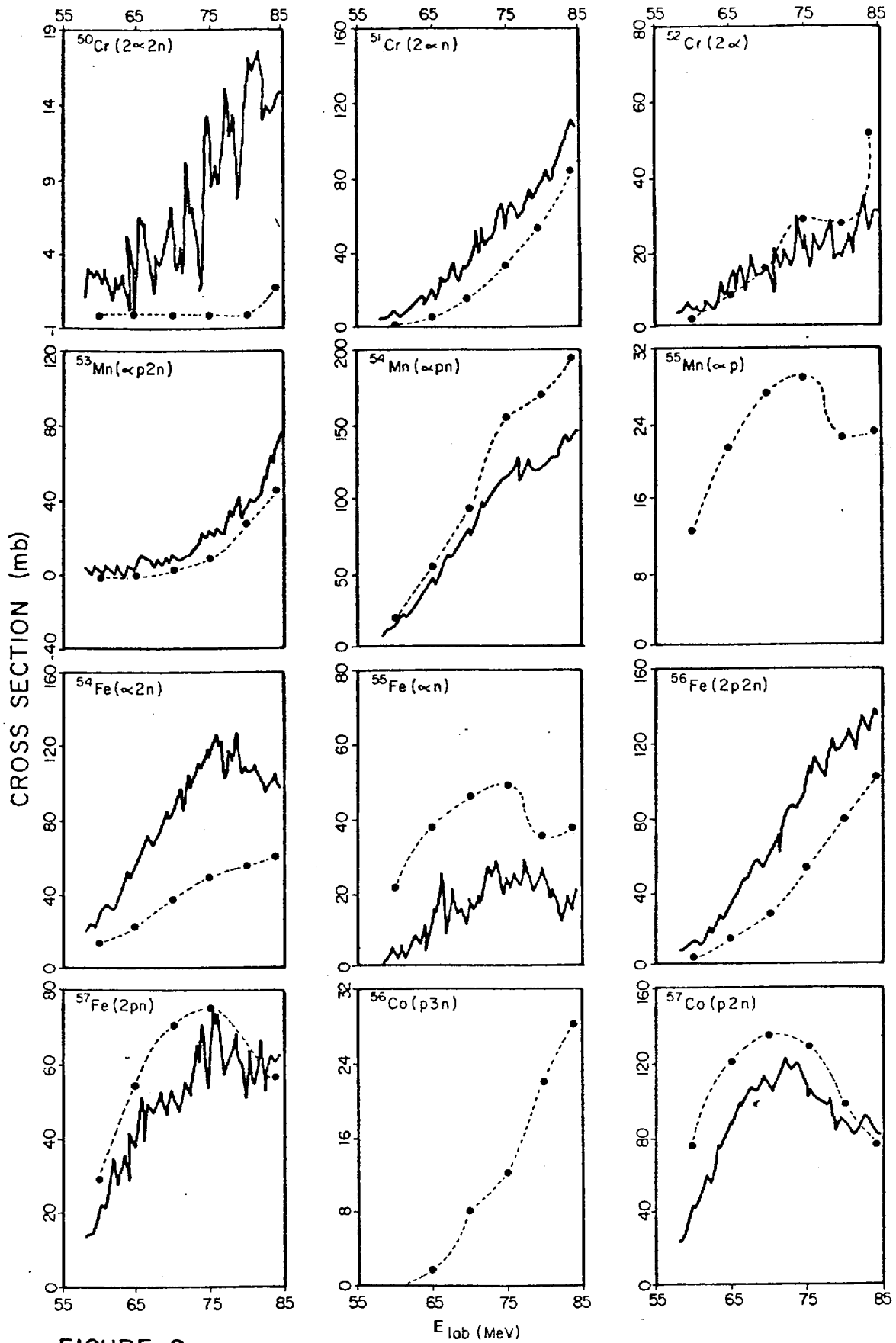


FIGURE 9